Experimental and Finite Element Analysis for Mechanics of Soil-Tool Interaction

A. Armin, R. Fotouhi, W. Szyszkowski

Abstract—In this paper a 3-D finite element (FE) investigation of soil-blade interaction is described. The effects of blade's shape and rake angle are examined both numerically and experimentally. The soil is considered as an elastic-plastic granular material with non-associated Drucker-Prager material model. Contact elements with different properties are used to mimic soil-blade sliding and soil-soil cutting phenomena. A separation criterion is presented and a procedure to evaluate the forces acting on the blade is given and discussed in detail. Experimental results were derived from tests using soil bin facility and instruments at the University of Saskatchewan. During motion of the blade, load cells collect data and send them to a computer. The measured forces using load cells had noisy signals which are needed to be filtered. The FE results are compared with experimental results for verification. This technique can be used in blade shape optimization and design of more complicated blade's shape.

Keywords—Finite element analysis, soil-blade contact modeling, blade force, experimental results.

I. INTRODUCTION

DEVELOPNIG self-ruling vehicles for agricultural tasks to help farmers is incentive of this study. About half of energy used for agricultural purposes is used operation which include soil-tool interaction (tillage operation), because of high draft blade force [1]. This consumed energy is because of the ineffient energy which transferred from blade to the soil [2]. Majority of tillage interaction studies have been focused to generate force calculation models by using different types of soil (different physical and mechanical Properties), blade (blade shape, blades' rake angle), and functional conditions (depth and width of cut, blade's travel speed, etc.) [3]. As shape of blade affects the soil failure's shape and subsequently changes forces on the blade, optimization of the blade shape will help increase energy efficiency. Based on the complex system, it is possible to only predict the force of simple rectangular blade shape based on analytical model. Therefore, design optimization cannot perform based on analytical method. Progress in computational techniques gives researchers the opportunity to develop highly efficient programs for handling real difficult situations by simulation [4]. By using Finite Element Method (FEM) and other numerical methods, appropriate constitutive (stress-deformation) relations for different working conditions are developed to help to analyze the tillage interaction. Several research studies and models have been accomplished based on FEM, such as [5]-[8]. In these papers, researchers predicted

Ahad Armin is with the Red Deer College, Canada (e-mail: ahad.armin@rdc.ab.ca).

responses of tools during soil-tool interaction by suggesting different FE models and simulating tillage interaction.

The general objective of this study is to develop a simulation technique for modeling the tillage interaction for all types of blade's shape. Simulation force results on the straight blades are compared with analytical results [9], [10]. Saskatchewan soil is selected for this research work.

II. CONSTITUTIVE LAW FOR SOIL

In this study, the soil-blade interaction is demonstrated by the Drucker-Prager criteria with a non-associate flow rule controlled by the rate of dilatancy angle v, which denotes the volumetric expansion and frictional-dilatancy behavior of the material.

If there is no volumetric expansion, then $v = 0$ (shear type of deformation only), which matches the direction 3 (vertical) of the increments of plastic strain in Fig. 1. On the other hand, for the flow rule related with criterion (1), the increments of plastic strains would have direction 1 that comprises shear deformation and dilatations considered by the dilatancy angle $v = \varphi$. According to [11], for real materials, angle v is typically less than φ and should be within the limits $0 < v < \varphi$ as shown by direction 2 (the values of factors used in the paper are listed in Table I).

In the Finite Element Analysis, the dotted curve in Fig. 1 is the material behavior defined by this law. It starts with elastic deformations until the yield criterion is reached and then the curve lines up with the yield surface (points are on this surface). Plastic deformations generated along the yield surface may be considered as compacting.

As the separation status in FE can only be defined at nodes, the simulated separation procedure is 'discrete' in this logic that there would be some stress relieve by changing node status from initially connected to separated. For instance, if just before the first departure the stress state is defined by T_1 then just after departure it will be lowered and back in the elastic region. In this area, the highest stress state, denoted by B_1, will be typically at the opening's tip, i.e. at the node to be separated next. Then after a more load increase (controlled here by the forced blade's displacement), the stress state is detected at the node that would separate next. Similar to the previous approach, this stress reaches the yield surface again and then follows by the surface until arriving at point T_2 where the separation happens again. After separating at the subsequent node, the stress state drops to B_2, and so on (points B_1, B_2 are further interpreted, discussed in detail and shown in [13]).
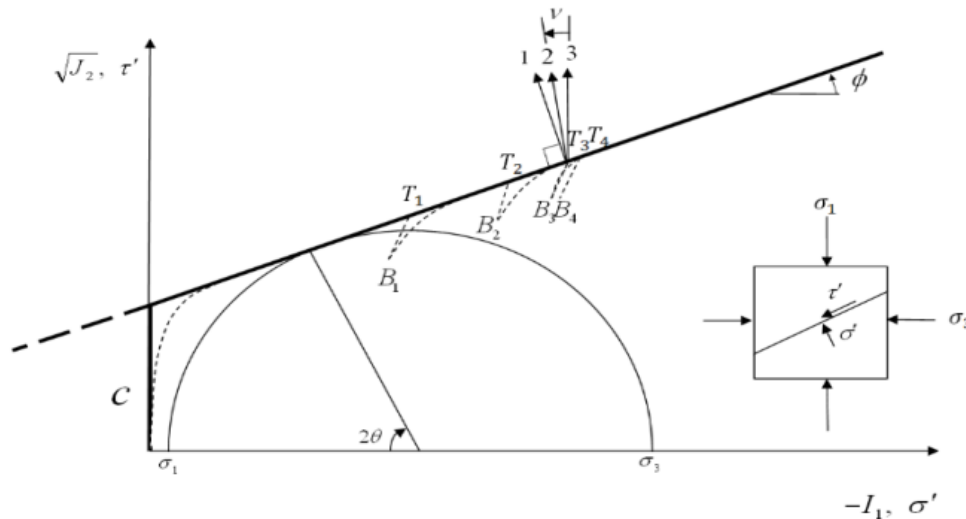
Fig. 1 The Drucker-Prager material law with non-associated flow rule

TABLE I
SOIL AND BLADE PARAMETERS USED IN PRESENT ANALYSIS

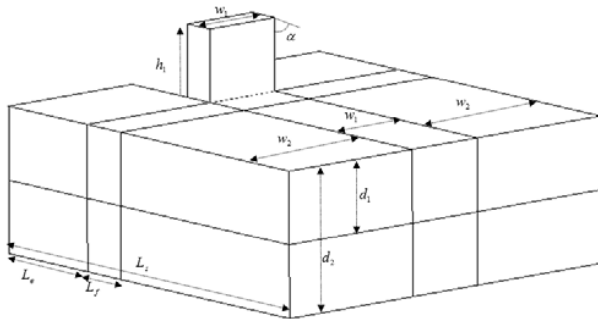| Properties	Soil	Blade
C- Cohesion	$20 Kpa$	
φ- Soil internal friction angle	$35°$	
v - Dilatancy angle	$20°$	
$\bar{\omega}$- Soil water content	7%	
E - Modulus of elasticity	$5\ Mpa$	$200000\ Mpa$
μ - Poisson's ratio	0.36	0.3
ρ - Density	$1220 \frac{Kg}{m^3}$	$7850 \frac{Kg}{m^3}$
φ_b - Blade-soil friction angle	$23°$	

Fig. 2 Parameters of the FE model

TABLE II
SOIL-TOOL MODEL DIMENSIONS USED IN FE ANALYSIS

$w_1(mm)$	$d_1(mm)$	$L_f(mm)$	$L_e(mm)$
50	50	50	100
$d_s(mm)$	$w_s(mm)$	$L_s(mm)$	α
150	300	300	90

III. MATERIAL AND METHODS

A. The FE Models

In the 3D FE model, SOLID45 hexahedral elements with 3 degree of freedom at each point are selected from library of elements in ANSYS to represent both soil and blade. The connection between soil and blade is modeled by the contact elements CONTACT173 and TARGET170. These contact elements are modeled along the departure surfaces as discussed in the next section. Based on the complexity of the system and large number of convergence equilibrium iteration, calculations generally last several hours. Thus, different meshing patterns were tested to balance between computational work and accuracy of calculations.

B. Model Description

Fig. 2 represents the geometry of FE model. As shown in this figure, the soil model dimension is L_S= 300 mm × w_S= 300 mm × d_S= 150 mm. In order to be able to mesh with different densities, the soil block is divided into several sub-blocks. The maximum distance blade can travel while cutting the soil, also the length of contacts between upper and lower blocks of soil, is L_f= 50 mm (this dimension will be justified later). Parameter w_1 is the width of cut soil (also the width of blade), w_2 is the side width of soil block. The depth of cut soil is d_1; which is also the cutting depth of blade. The angle between blade and soil is defined by α, the rake angle. Soil block dimensions are listed in Table II.

C. The Separation Criterion

By helping contact elements, the elements along the expected departure surface are connected at nodes. The element at the tip of the opening has the highest stress/deformation level. By motion of the blade through the soil, stresses go through the elastic phase (see the broken line in Fig. 1) until it reaches the solid line, yielding condition (1). Strain component ε_x is monitored continuously in the element at the tip of blade. This monitoring will continue until $\varepsilon_x = \varepsilon_c$. At this instant, force attachment of the nodes at the opening's tip (of the tip element) are deactivated, and it creates the first opening or separation. This is also associated with relieving the stresses to the state denoted by point B_1, and a lower value of ε_x below ε_c (limiting compacting strain).By further motion of blade, the stress state will be increasing to reach the yielding state again. The strain ε_x will

become equal to ε_c at T_2 and separation took place similar to the last step. The separation criterion, calculating forces on the blade and numerical experimentation to set a predefined magnitude of ε_c are explained in details in [13].

D. Experimental Setup

In order to find out horizontal force acting on the blade during the motion of blade through the soil, actual experiments were performed using a linear monorail system in the soil bin. This monorail system is capable of moving tools inside the soil at different speeds. A picture of the soil bin is presented in Fig. 3 (12 m length by 1.8 m wide, 9 m moveable length). The tool carriage is equipped with six S-type load cells (2 horizontal, 3 vertical, and 1 side). This makes measurement of the force acting on the blade in three directions. The blade has a rectangular shape with size of $54cm \times 4cm \times 2cm$ was attached to the main frame as shown in Fig. 4. For this experiment we used Saskatchewan soil with 7% water content as given in Table I [14].
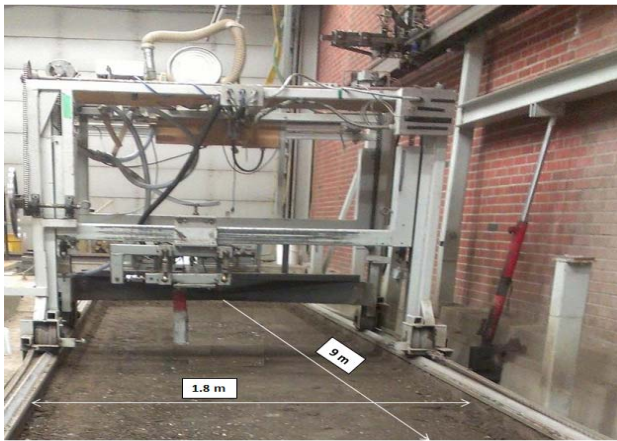
E. Experimental Procedure

According to [15], for narrow blades, the effect of blade speed on the blade force is negligible if the speed is less than $\sqrt{5g(w + 0.6d_1)}$; where g and w represent gravitational acceleration and width of the blade respectively. For a blade with $W = 0.04\,m, g = 9.81\,{}^m/_{s^2}$, and $d_1 = 0.05\,m$, the speed is $1.85\,{}^m/_s$ (6.7 ${}^{km}/_h$). All the tests were performed at a speed of 2 km/h. The blade size and depth of blade inside the soil for these experiments were identical to those used in the FE simulations. Each experiment started after placing the blade at the required depth. Fig. 5 shows horizontal force on the blade, which are measured by summing of the two horizontal load cells. During motion of the blade inside the soil, load cells collect information at every 2.5 milliseconds and send them to a computer. The measured force on the blade was a noisy signal as shown in Fig. 5.
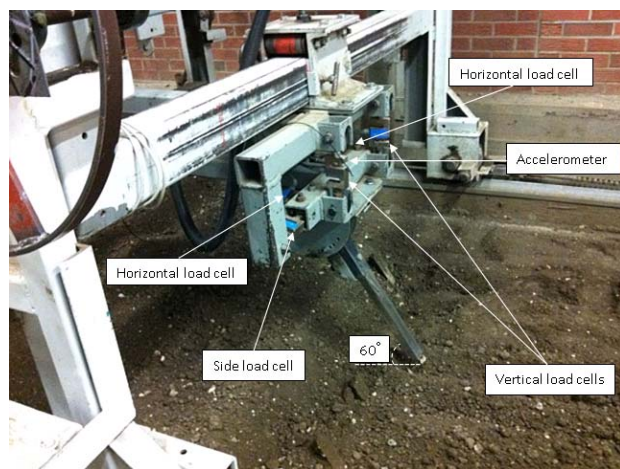

Fig. 3 The soil bin at the University of Saskatchewan (12 m long and 1.8 m wide)

Fig. 4 The blade with $60°$ rake angle attached to the linear monorail system for test
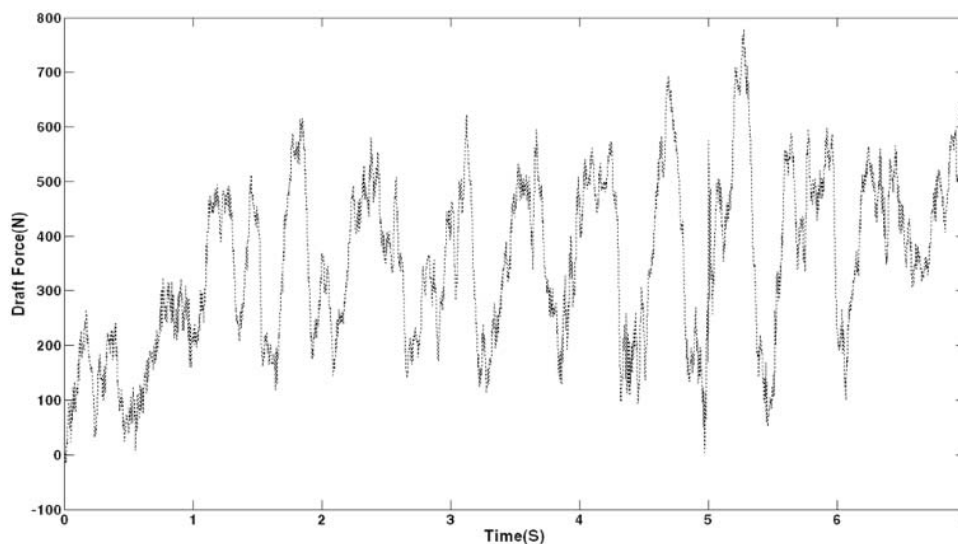

Fig. 5 Unfiltered horizontal (draft) force on the blade when moving with rake angle

In order to figure out what frequencies should be filtered out, the natural frequencies of the blade attached to the monorail (with its tip inside the soil) were calculated using two different measurements (first signal from horizontal load cells, and second signal using an accelerometer attached to the monorail system as shown in Fig. 4) and applying Fast Fourier Transform (FFT). Figs. 6 and 7 show natural frequencies of the system using FFT of the signals from accelerometer and horizontal load cells, respectively. As it can be seen from these figures, the first two natural frequencies are about 21 and 38 Hz, respectively. Then frequencies of the system (monorail and frame) were calculated using similar measurements and FFT when the blade was moving inside the soil with speed of 2 km/h.
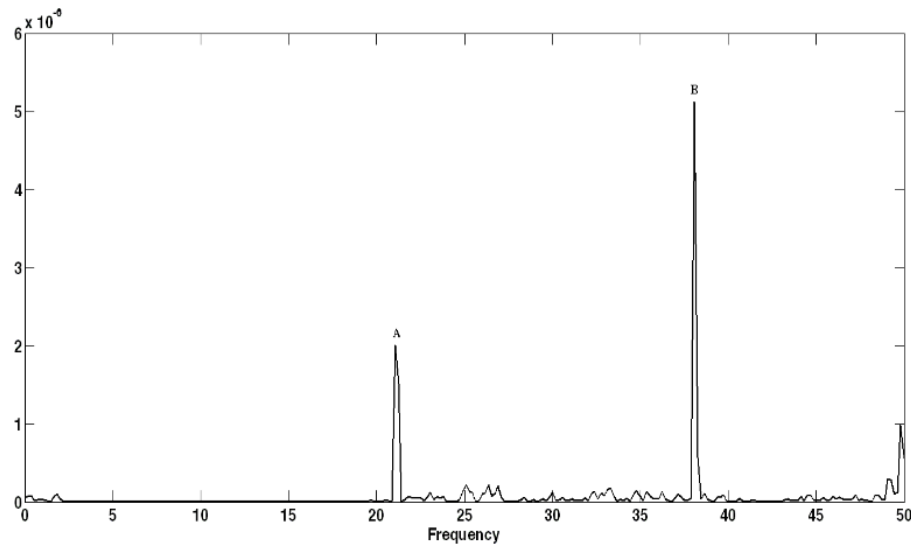

Fig. 6 The natural frequencies of system: using FFT of the signal from accelerometer (A=21.06, B=38.09)
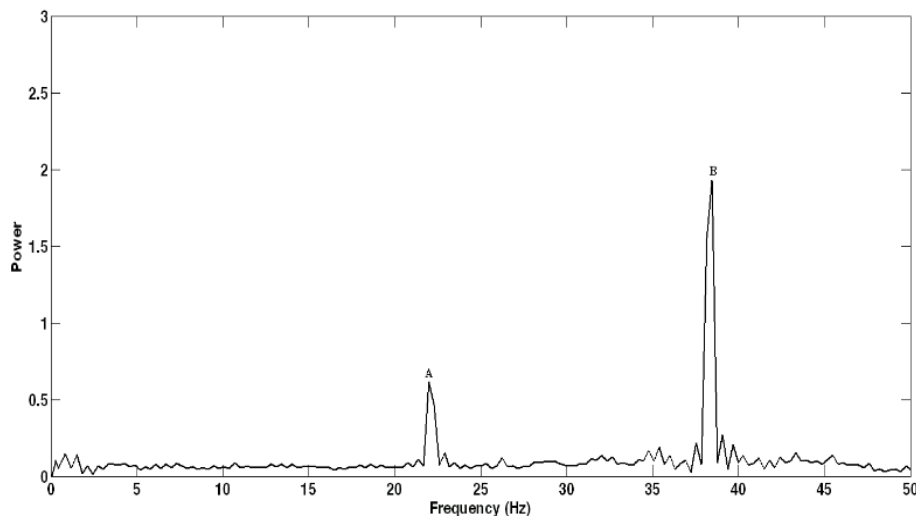

Fig. 7 The natural frequencies of system: using FFT of the signal from horizontal load cells (A=21.97, B=38.45)

Figs. 8 and 9 show frequencies of the system, when blade was moving inside the soil using FFT of signals from accelerometer and horizontal load cells, respectively. As can be seen from these figures, the first three frequencies are about 1.5, 21 and 40 Hz. Comparing these forced frequencies with the natural frequencies (21 and 38 Hz), it can be concluded that 1.5 Hz is the forced frequency and the other two (21 and 40) are natural frequencies of the system. In order to exclude the effect of natural frequencies, we filtered out all frequencies above 2Hz from the signal representing force of the blade.

F. Validation of the FE Model

A typical plot of the blade force calculated by the procedure presented in Section D is shown in Fig. 10 for 3D soil-blade interaction. This is the case with $\alpha = 60°$ and $d_1 = 50 \, mm$, and $w_1 = 40 \, mm$, modeled by the mesh with the element size $e = 7 \, mm$ (as discussed in [13]). As shown in

Fig. 10, the average force $\bar{F}$ is almost horizontal after the first iteration already, and the corresponding blade force is $F_D = $ 408 N.
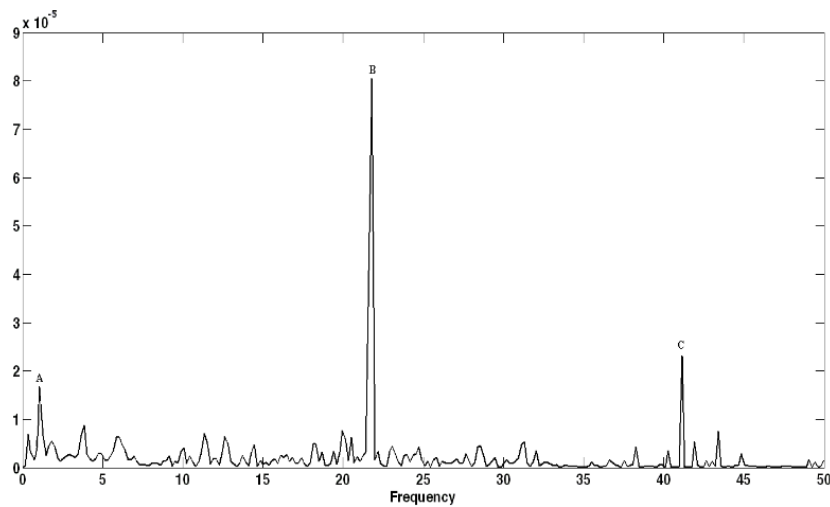

Fig. 8 The frequencies of the system when blade is moving inside the soil with 2 km/h, using measurement signal from accelerometer (A=1.1, B=21.7, C=41.2)
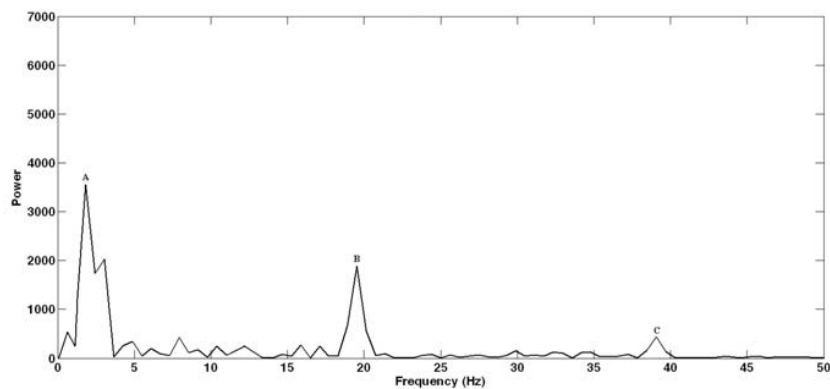

Fig. 9 The frequencies of the system when blade is moving inside the soil with 2 km/h, using measurement signal from horizontal load cells (A=1.8, B=19.5, C=39.0)
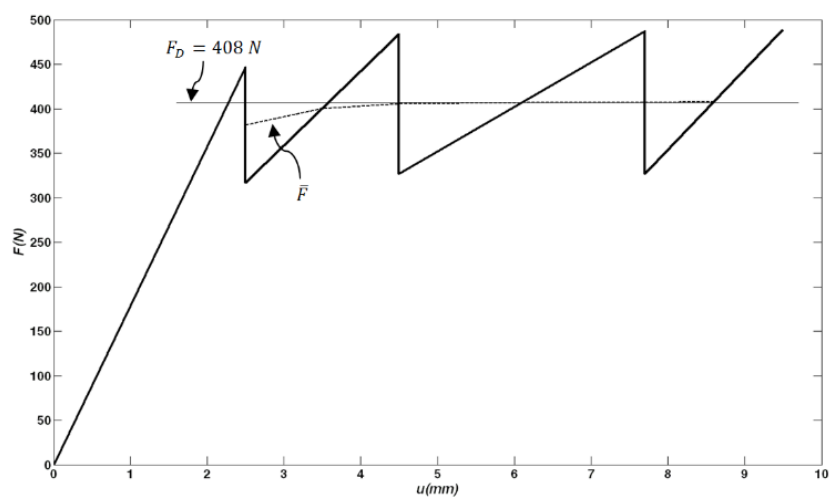

Fig. 10 The force acting on the blade and its mean value (draft force F_D)

FE results can be validated by comparing with the analytical and experimental blade force result. For analytical results, McKeyes [12] proposed (1) for a narrow blade:

$$P = (\gamma d_1^2 N_\gamma + C d_1 N_c + Q d_1 N_q) w_1 \qquad (1)$$

where P is the total force, γ is soil specific weight, C is soil cohesion, Q is bearing pressure (due to soil accumulation), d_1 is cutting depth of the blade and (N_γ, N_c, N_q) are cutting factors for narrow blade. (N_γ, N_c, N_q) are parameters that depend on the soil friction angle $\emptyset$, and the blade rake angle α. In the present study, the value of Q is negligible (for narrow blades) and horizontal components of $(N_{\gamma H}, N_{cH})$ for obtaining draft forces are derived from McKeyes [10] for different values of these variables as shown in Table III. Here $Q d_1 N_q \approx 0$ for narrow blades.

TABLE III
ANALYTICAL RESULTS: HORIZONTAL COMPONENT OF CUTTING FACTORS FOR OBTAINING HORIZONTAL DRAFT FORCE ON THE BLADE

Rake angle (α)	w_1/d_1	$N_{\gamma H}$	N_{cH}
60	0.8	6.94	10.42

It is known that depth of interaction, width of blade and rake angle have primary effects on the results that by increasing each of them, draft forces will be increased. By applying (1) and considering model parameters, which are presented in Table IV, draft force on the blade can be determined.

TABLE IV
ANALYTICAL RESULTS: SOIL AND BLADE PARAMETERS

Rake angle (°)	$w_1(m)$	$d_1(m)$	$\gamma (\frac{N}{m^3})$	C (KPa)	$N_{\gamma H}$	N_{cH}
60	0.04	0.05	12000	20000	6.94	10.42

$$P_H = (\gamma d_1^2 N_{\gamma H} + C d_1 N_{cH}) w_1$$
$$P_H = 425N$$

The difference in total horizontal blade force between FE results (using regular mesh density model, $F_D = 408N$), and analytical result is found to be about 4%; this can be considered as validation of our FE results. On the other hand, as mentioned in Section F, the experimental force result signal was filtered to exclude all frequencies above 2 HZ as shown in Fig. 11. The filtered blade force increased sharply at the first of interaction between soil and blade and stayed almost constant for the rest and is around 415 N.
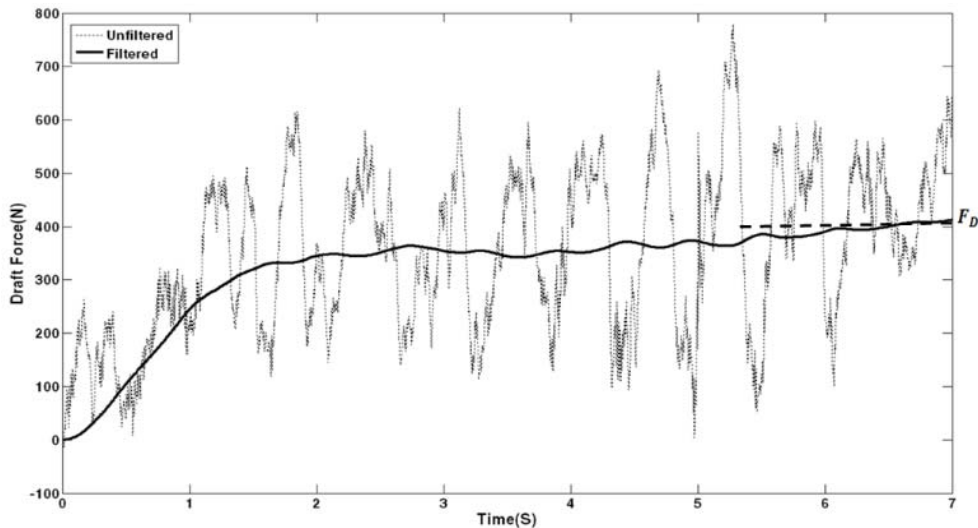

Fig. 11 Experimental results: Horizontal force on the blade when blade moves inside the soil with speed of 2 km/h (Filtered: all frequencies over 2 HZ are filtered out)

TABLE V
COMPARING THE EXPERIMENTAL, ANALYTICAL, AND FE RESULTS

$d_i(m)$	$w_i(m)$	Analytical force, $F_D(N)$	FE force, $F_D(N)$	Experimental Force, $F_D(N)$
50	40	425.0	408.0	415
Difference between analytical and experimental (%)			Difference between FE and experimental (%)	
2.3			1.6	

The experimental results are compared with the analytical and FE results as shown in Table V. The difference between analytical and experimental results is 2.3%, and the difference

between FE and experimental results is 1.6% which shows good correlations between these three methods. Therefore our FE model is validated with both analytical and experimental ones.

IV. CONCLUSION

A technique for simulating the soil-blade interaction by the FEM is presented. The procedure is based on the non-associated Drucker-Prager constitutive law with a compaction strain based departure criterion to define the behavior of soil being cut by the blade. Several surfaces (separation and

sliding) are defined in this investigation. The elements on these faces are attached to each other by special help of contact elements. By movtion of the blade through soil, the attachment along the departure surfaces is allowed to break resulting in departure of the soil elements.

During experiment in the soil bin, by moving the blade through the soil, load cells which are attached to the monorail, sensed the force acted on the blade from the soil. It was shown that the analyzed force based on collected data were very noisy. In order to figure out what frequencies should be filtered out, natural frequencies of the blade attached to the monorail and force frequencies of the system were calculated using two different measurements.

The simulation results show a good correlation with the semi-analytical formulas of the classical soil mechanics and filtered experimental results.

It is hoped that the technique presented can be extended to the investigation of any arbitrary shape of blades, which result in the tillage optimization.

REFERENCES

[1] Zhang, J., and Kushwaha, R.L. 1998, "Dynamic analysis of tillage tool: Part I – Finite element method", Canadian Agriculture Engineering; Vol (40), pp. 287-292.

[2] Ashrafi Zadeh, S.R, 2006. "Modeling of energy requirements by a narrow tillage tool'. Unpublished Doctoral Thesis at the University of Saskatchewan, Saskatoon, Canada.

[3] S.Karmakar, 2008, "Modeling of soil-tool interaction in tillage". Transworld research network, India.

[4] M. Abo-Elnor, R. Hamilton, J.T. Boyle, 2004, "Simulation of soil-blade interaction for sandy soil using advanced 3D finite element analysis", Soil & Tillage Research. Vol(75), pp. 61-73.

[5] J. Wang, and D. Gee-Clough, 1991, "Deformation and failure in wet clay soil. Simulation of tine soil cutting". Proc IAMC Conference Beijing, China. Pp. 219-226.

[6] L. Chi, and R.L. Kushwaha, 1989, "Finite element analysis of force on a plane soil blade". Canadian Agriculture Engineering, Vol(31), pp. 135-140.

[7] J. Shen, and R. L. Kushwaha, 1998, "Soil-Machine Interactions-A Finite Element Perspective", Marcel Dekker Inc. Publishers,.

[8] S.K. Upadhyaya, U.A. Rosa, and D. Wulfsohn, 2002, "Application of the finite element method in agricultural soil mechanics", Advances in soil Dynamics, PP. 117-153.

[9] D.R.P. Hettiaratchi, A.R., Reece, The calculation of passive soil resistance. Computers and Geotechnique. 24 (1974) 280-310.

[10] E. McKyes, O.S. Ali, The cutting of soil by a narrow blade. Journal of Terramechanics. 14 (1977) 43-58.J. Shen, and R. L. Kushwaha, 1998, "Soil-Machine Interactions-A Finite Element Perspective", Marcel Dekker Inc. Publishers,.

[11] Y. Chen, L. J. Munkholm, T. A. Nyord, Discrete element model for soil-sweep interaction in three different soils. Soil & Tillage Research. 126 (2013) 34-41.

[12] E. McKeyes, Soil cutting and tillage. Elsevier Science Publishing Company, New York, 1985.

[13] A. Armin, R. Fotouhi, W. Szyszkowski, On the FE modeling of soil–blade interaction in tillage operations, Finite elements in analysis and design 92(2014)1-11.

[14] A. Bankole, Critical State Behaviour Of An Agricultural Soil. Doctoral Thesis at the University of Saskatchewan, Saskatoon, Canada, 1996.

[15] Godwin, R.J., O'Dogherty, M.J. Integrated soil tillage force prediction models. Journal of Terramechanics; 44(2007) 3-14